Pergamon

Mathl. Comput. Modelling Vol. 19, No. 1, pp. 59–70, 1994

0895-7177/94 $6.00 + 0.00

0895-7177(94)E0007-A

Mathematical Modelling of Blood Flow Through an Overlapping Arterial Stenosis

S. CHAKRAVARTY AND P. K. MANDAL
Department of Mathematics
Visva-Bharati University, Santiniketan 731 235, India

(Received June 1993; accepted July 1993)

Abstract—Of concern in the paper is a theoretical study of blood flow in an arterial segment in the presence of a time-dependent overlapping stenosis using an appropriate mathematical model. A remarkably new shape of the stenosis in the realm of the formation of the arterial narrowing caused by atheroma is constructed mathematically. The artery is simulated as an elastic (moving wall) cylindrical tube containing a viscoelastic fluid representing blood. The unsteady flow mechanism of the present investigation is subjected to a pulsatile pressure gradient arising from the normal functioning of the heart. The equations governing the motion of the system are sought in the Laplace transform space and their relevant solutions supplemented by the suitable boundary conditions are obtained numerically in the transformed domain through the use of an appropriate finite difference technique. Laplace inversion is also carried out by employing numerical techniques. A thorough quantitative analysis is performed at the end of the paper for the flow velocity, the flux, the resistive impedances, and the wall shear stresses together with their variations with the time, the pressure gradient, and the severity of the stenosis in order to illustrate the applicability of the present mathematical model under consideration.

INTRODUCTION

The study of blood flow through arteries under stenotic conditions is believed to be one of the most serious physiological problems because of the fact that the cause and development of many vascular diseases leading to the malfunction of the cardiovascular system have a close relationship with the nature of blood movement and the deformability of the vascular wall. The common form of arterial narrowing or stenosis is that caused by atheroma, a deposition of fats and fibrous tissue in the arterial lumen. Such constriction of the arterial lumen grows inward and restricts the normal movement of blood where the transport of blood to the region beyond the narrowing is reduced considerably. Moreover, under normal physiological condition, the transport of blood in the human circulatory system depends entirely on the pumping action of the heart which produces a pressure gradient throughout the arterial system.

Quite a good number of theoretical studies related to blood flow through arteries in the presence of a single stenosis have been carried out in the recent past [1–5]. These studies have all assumed the flow of the blood to be Newtonian and that the stenosis could be represented by a mathematical function viz. the cosine function. However, it has been observed from experimental investigations that blood, being a suspension of cells, behaves like a non-Newtonian fluid at low shear rates in smaller arteries [6–10]. The effects of mild stenosis on the resistive impedance and the wall shear stress in an artery have been put forward by Shukla *et al.* [11] who considered the flowing blood to be non-Newtonian characterized by the Power law and Casson's fluid models.

The authors are grateful to the Council of Scientific and Industrial Research for providing the financial support in the present work.

In the light of this aspect, several analytical studies [12–14] have been carried out in order to quantify the effects of stenosis on the flow characteristics of blood, the resistance to flow and the wall shear stress. Although the experimental studies [15,16] indicate that human blood possesses significant viscoelastic properties in the frequency range of physiological importance, very little is known about the unsteady flow of a viscoelastic fluid produced by a pulsatile pressure gradient arising from the normal functioning of the heart. The viscoelastic properties of blood may be attributed to several factors. The dominant factors are the viscoelastic properties of individual red cells and the internal structures formed by cellular interactions. The influence of the elastic behaviour of the individual red cell suspensions has been examined by several investigators theoretically as well as experimentally. In most of the recent studies related to stenotic flow either in a rigid vessel or in a deformable artery, the stenotic geometry has been regarded as time-independent. This may suit well for a rigid vessel, but for a flexible arterial wall, the stenosis cannot remain static. Moreover, the studies mentioned above have dealt with the arterial flow in the presence of a single (mild) stenosis. Perhaps it would be more interesting to study the effects of overlapping stenosis in the realm of the formation of the arterial narrowing on the flow characteristics of blood which would be of great help to the bioengineers who are engaged in the design and the construction of improved artificial organs.

With the above discussion in mind, we propose to study the unsteady flow behaviour of blood in an artery under stenotic condition analytically, by considering blood to be non-Newtonian fluid and by properly accounting for blood viscoelasticity while the shape of the stenosis has been chosen to be overlapped to some extent depending on time. The arterial segment under consideration is taken to be an elastic cylindrical tube in which the flow is governed by a pulsatile pressure gradient owing to the normal functioning of the heart. Although this general problem is of great interest, the prime attention is focussed in the present investigation on the effect of wall motion on local fluid mechanics and not on the stresses and strains in the arterial wall per se. A suitable time-dependent geometry of a new overlapping stenosis has been constructed and duly accounted for in order to have the dynamic response of the stenosed arterial system under an *in vivo* situation. The cylindrical coordinate system has been taken for the analytical formulation. The governing equations of motion for the system are sought first in the Laplace transform space and their solutions are obtained subject to the suitable boundary conditions with the use of a finite difference scheme. Using the central difference formula and performing the Thomas algorithm, the flow velocity of blood, the flux, the resistive impedance, and the wall shear stress are obtained in the transformed domain. Laplace inversion is carried out finally by employing Gauss quadrature formula. A thorough quantitative analysis is performed at the end of the paper for the desired quantities through the exhibition of their results graphically followed by a complete discussion. The present investigation, it is believed, will certainly have potential applications in the proper design and construction of appropriate artificial organs.

FORMULATION OF THE PROBLEM

The stenosed artery under consideration is modelled as a thin elastic circularly cylindrical tube containing a viscoelastic fluid representing blood. Let (r, θ, z) be the coordinates of a material point in the cylindrical polar coordinate system in which the z-axis is taken along the axis of the artery, while r and θ are taken along the radial and the circumferential directions, respectively.

The newly constructed time-dependent geometry of the overlapping stenosis (Figure 1) which is assumed to be manifested in the lumen of the arterial segment, may be described by

$$\frac{R(z,t)}{a} = 1 - a_1(t)\left[\frac{11}{32}(z-d)l_0^3 - \frac{47}{48}(z-d)^2 l_0^2 + (z-d)^3 l_0 - \frac{1}{3}(z-d)^4\right], \quad d \le z \le d + \frac{3l_0}{2}, \tag{1}$$

$$= 1, \qquad \text{otherwise,}$$

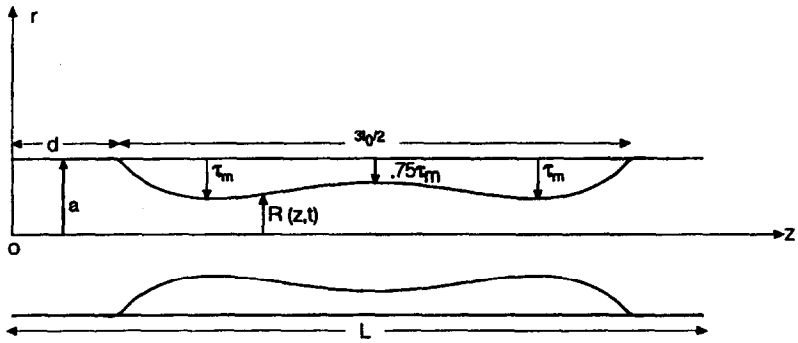

Figure 1. The geometry of the overlapping stenosis in an artery.

where $R(z,t)$ is the radius of the arterial segment in the stenotic region, a is the constant radius of the normal artery in the nonstenotic region, $3l_0/2$ is the length of the stenosis, and d indicates the location of the stenosis. The time-dependent parameter $a_1(t)$ is given by

$$a_1(t) = \frac{32}{4al_0^4}\tau_m\left(1 - e^{-t/T}\right), \tag{2}$$

in which the maximum height τ_m of the stenosis appears at two specific locations of $z = d + l_0/2$ and $z = d + l_0$ such that the ratio of the height of the stenosis to the radius of the normal artery is much smaller than unity. Also the height of the stenosis at a distance of $d + 3l_0/4$ from origin is chosen to be $3\tau_m/4$. The arterial segment under consideration is taken to be of finite length L. Here T designates a time parameter.

Let us consider the stenotic blood flow to be unsteady, axisymmetric, laminar, one-dimensional, and fully developed. The basic equation of motion governing such flow (in the absence of any radial/rotational flow, and taking into account the experimental observation that when the shear rate is not too high, whole blood exhibits non-Newtonian behaviour) may be written as

$$\rho\frac{\partial w}{\partial t} = \mu^*\left(\frac{\partial^2 w}{\partial r^2} + \frac{1}{r}\frac{\partial w}{\partial r}\right) - \frac{\partial p}{\partial z}, \tag{3}$$

where $w = w(r,z,t)$ is the axial velocity of the flowing blood, p is the pressure, ρ is the density, and μ^* is the complex viscosity of blood, defined by

$$\mu^* = \int_0^\alpha \frac{F(\tau)}{1 + i\omega\tau}\,d\tau, \tag{4}$$

in which $F(\tau)$ represents the relaxation function characterizing the viscoelastic behaviour of the flowing blood whose form may be chosen as

$$F(\tau) = \mu\left(\frac{t_2}{t_1}\right)\delta(\tau) + \mu\left(\frac{(t_1 - t_2)}{t_1}\right)\delta(\tau - t_1), \tag{5}$$

where t_1 is the relaxation time, μ is the constant viscosity, t_2 is the retardation time, and ω represents the angular frequency. For small shear rate, t_1 and t_2 may be assumed to be small.

Since the consideration of the axial flow is of our prime concern, we further have

$$\frac{\partial p}{\partial r} = 0 = \frac{\partial p}{\partial \theta}. \tag{6}$$

These relations yield $p = p(z,t)$. The form of the pressure gradient $\dfrac{\partial p}{\partial z}$ present in (3) appearing due to pumping action of the heart, has been taken from [17] as

$$\frac{\partial p}{\partial z} = A_0 + A_1\cos(\omega t), \tag{7}$$

where A_0 is the constant amplitude of the pressure gradient, A_1 is the amplitude of the pulsatile component giving rise to systolic and diastolic pressure; $\omega = 2\pi f_p$, and f_p is the pulse frequency.

BOUNDARY CONDITIONS

The velocity gradient of the streaming blood along the axis of the arterial segment may be assumed to be equal to zero; that means, there is no shear rate of the fluid along the axis, which may be written as

$$\frac{\partial w}{\partial r} = 0, \qquad \text{on } r = 0. \tag{8}$$

The velocity boundary condition on the arterial wall is the usual no-slip condition, given by

$$w = 0, \qquad \text{on } r = R(z,t). \tag{9}$$

Also, it is assumed that there is a nonzero velocity of the flowing blood when the system is at rest. That means,

$$w = w_0, \qquad \text{at } t = 0. \tag{10}$$

METHOD OF SOLUTION

Usually in a problem involving coupling of the fluid mechanics with the vessel wall mechanics, $R(z,t)$ would not be given but instead, could be computed as part of the solution of the coupled problem. Here, we consider $R(z,t)$ as prescribed and, hence, our attention is focussed on the hemodynamic factors.

Let us introduce a radial coordinate transformation as an initial step, given by

$$\xi = \frac{r}{R(z,t)}, \tag{11}$$

which has the effect of immobilizing the arterial wall in the transformed coordinate ξ. Incorporating this transformation, the equation of motion (3) takes the following form

$$\rho\frac{\partial w}{\partial t} = \mu^*\left[\frac{1}{R(z,t)^2}\frac{\partial^2 w}{\partial \xi^2} + \frac{1}{\xi R(z,t)^2}\frac{\partial w}{\partial \xi}\right] - \frac{\partial p}{\partial z} + \frac{\rho\xi}{R(z,t)}\frac{\partial R}{\partial t}\frac{\partial w}{\partial \xi}. \tag{12}$$

The boundary conditions (8)–(10) are also transformed in concert with (11) to

$$\frac{\partial w}{\partial \xi} = 0, \qquad \text{on } \xi = 0, \tag{13}$$

$$w(\xi, z, t) = 0, \qquad \text{at } \xi = 1, \qquad \text{and} \tag{14}$$

$$w(\xi, z, t) = w_0, \qquad \text{at } t = 0. \tag{15}$$

The last term appearing on the right hand side of (12) is associated with the arterial wall motion. Now to solve this equation governing the motion of the system supplemented by the boundary conditions (13)–(15), these are all sought on the Laplace transform (L.T.) space which are read as

$$\frac{\mu^*}{\bar{R}^2}\left[\frac{\partial^2 \bar{w}}{\partial \bar{\xi}^2} + \frac{1}{\bar{\xi}}\frac{\partial \bar{w}}{\partial \bar{\xi}}\right] + \frac{\rho\bar{\xi}}{\bar{R}}\left[s\bar{R} - R(z,0)\right]\frac{\partial \bar{w}}{\partial \bar{\xi}} - \rho s\bar{w} = \frac{d\bar{p}}{dz} - \rho w(\bar{\xi}, z, 0), \tag{16}$$

accompanied by the transform boundary conditions in the L.T. space

$$\frac{\partial \bar{w}}{\partial \bar{\xi}} = 0, \qquad \text{on } \bar{\xi} = 0, \qquad \text{and} \tag{17}$$

$$\bar{w} = 0, \qquad \text{on } \bar{\xi} = 1, \tag{18}$$

where the quantities designated by a bar represent their Laplace transforms and s is the transformation variable.

FINITE DIFFERENCE APPROXIMATION

The finite difference scheme for solving equation (16) is based on the central difference formula to transform all the spatial derivatives in the Laplace transform space in the following manner

$$\frac{\partial \bar{w}}{\partial \bar{\xi}} = \frac{\bar{w}_{i+1,j} - \bar{w}_{i-1,j}}{2\Delta\xi} \quad \text{and} \quad \frac{\partial^2 \bar{w}}{\partial \bar{\xi}^2} = \frac{\bar{w}_{i+1,j} - 2\bar{w}_{i,j} + \bar{w}_{i-1,j}}{(\Delta\xi)^2}.$$

The spatial derivatives of (16) are replaced by these finite difference representations so that the differential equation (16) may be transformed to the following difference equation:

$$\left[\frac{\mu^*}{\rho\bar{R}_j^2}\left\{\frac{1}{(\Delta\xi)^2} + \frac{1}{2\bar{\xi}\Delta\xi}\right\} + \frac{\bar{\xi}_i}{2\bar{R}_j\Delta\xi}\left(-a + s\bar{R}_j\right)\right]\bar{w}_{i+1,j} - \left[\frac{2\mu^*}{\rho\bar{R}_j^2(\Delta\xi)^2} + s\right]\bar{w}_{i,j}$$
$$+ \left[\frac{\mu^*}{\rho\bar{R}_j}\left\{\frac{1}{(\Delta\xi)^2} - \frac{1}{2\bar{\xi}\Delta\xi}\right\} - \frac{\bar{\xi}_i}{2\bar{R}_j\Delta\xi}\left(-a + s\bar{R}_j\right)\right]\bar{w}_{i-1,j} = \frac{1}{\rho}\frac{d\bar{p}}{dz} - w_0. \quad (19)$$

The above equation can be rewritten in a more compact form as

$$a_{i,j}\,\bar{w}_{i-1,j} + b_{i,j}\,\bar{w}_{i,j} + c_{i,j}\,\bar{w}_{i+1,j} = d_{i,j}, \quad (20)$$

in which

$$a_{i,j} = \frac{\mu^*}{\rho\bar{R}_j^2}\left\{\frac{1}{(\Delta\xi)^2} - \frac{1}{2\bar{\xi}\Delta\xi}\right\} - \frac{\bar{\xi}_i}{2\bar{R}_j\Delta\xi}\left(-a + s\bar{R}_j\right),$$
$$b_{i,j} = -\frac{2\mu^*}{\rho\bar{R}_j^2(\Delta\xi)^2} - s,$$
$$c_{i,j} = \frac{\mu^*}{\rho\bar{R}_j^2}\left\{\frac{1}{(\Delta\xi)^2} + \frac{1}{2\bar{\xi}\Delta\xi}\right\} + \frac{\bar{\xi}_i}{2\bar{R}_j\Delta\xi}\left(-a + s\bar{R}_j\right), \quad \text{and}$$
$$d_{i,j} = \frac{1}{\rho}\frac{d\bar{p}}{dz} - w_0.$$

Equation (20) is of the tridiagonal type and it can be solved by Thomas algorithm [18], where we define $\xi_i = (i-1)\Delta\xi$, $(i = 1, 2, 3, \ldots, N+1)$ and $z_j = (j-1)\Delta z$, $(j = 1, 2, 3, \ldots, M+1)$ for the entire arterial segment under consideration in which $\Delta\xi$ and Δz are the increments in the radial and the axial directions, respectively. Also, the boundary conditions (17) and (18) have their finite difference representations, given by

$$\bar{w}_{i,j} = \bar{w}_{2,j}, \quad \text{and} \quad (21)$$
$$\bar{w}_{N+1,j} = 0. \quad (22)$$

After having obtained the axial velocity $\bar{w}_{i,j}$ in the transformed space, the volumetric flow rate $\bar{Q}_j$ in the L.T. space can be determined as

$$\bar{Q}_j = 2\pi\bar{R}_j^2\int_0^1 \bar{\xi}_i\bar{w}_{i,j}\,d\bar{\xi}_i. \quad (23)$$

Finally, the resistance to flow $(\bar{\lambda}_j)$ and the wall shear stress $(\bar{\tau}_{rz})_j$ in the Laplace transform domain can be obtained as

$$\bar{\lambda}_j = L\frac{d\bar{p}/dz}{\bar{Q}_j}, \quad \text{and} \quad (24)$$
$$\left(\bar{\tau}_{rz}\right)_j = \mu^*\frac{\bar{w}_{N,j}}{\bar{R}_j\Delta\xi}. \quad (25)$$

Knowing all the solutions in the Laplace transform domain, the inversion is performed numerically by means of Gaussian quadrature formulae [19], in order to obtain measurements quantitatively and then interpret them physically with proper justifications, whenever necessary.

NUMERICAL RESULTS AND DISCUSSION

In this section, we shall discuss the applicability of the mathematical model and its analysis presented in the previous sections. For this purpose, we have made use of the available experimental data for the various physical parameters encountered in the present analysis. The numerical computations have been performed with the aim of examining the dynamic behaviour of the velocity profile, the flux, the resistive impedance, and the wall shear stress with a variation of the pressure gradient, the pulse frequency, and with various severity of the stenosis. For the purpose of numerical computations of the desired quantities concerned, and in order to have a thorough quantitative analysis, the following data have been made use of [20–22]: $a = 0.8\,\text{mm}$, $\rho = 1.024 \times 10^3\,\text{Kg/m}^3$, $L = 30\,\text{mm}$, $l_0 = 15\,\text{mm}$, $d = 4.5\,\text{mm}$, $\tau_m = 0.4a$, $A_0 = 500\,\text{Kg m}^{-2}\text{s}^{-2}$, $A_1 = 0.2A_0$, $f_p = 1.2\,\text{Hz}$, $T = 1\,\text{s}$, $\mu^* = (0.01 + 0.05i)$ Poise.

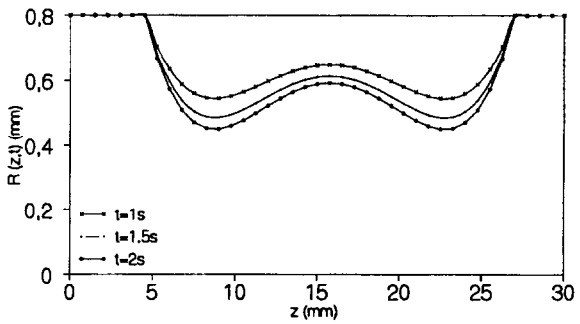

Figure 2. Geometrical shape of the stenosis with varying time ($T = 1\,\text{s}$) ($\tau_m = 0.4a$, $l_0 = 15\,\text{mm}$).

In order to have a clear understanding of the nature of the time-dependent overlapping stenosis present in the arterial lumen under consideration, the distributions of stenosis over the arterial segment are shown graphically in Figure 2 for different time periods. Three different curves correspond to the distributions of the shape of the stenosis for three different times whose concavity develops with the increasing time-scale. Hence, the fact that the stenosis varying considerably with time plays a significant role in studying the dynamic response of the flow behaviour of blood through the stenosed arterial system.

Numerical results obtained for the axial flow velocity by solving the difference equation (20) with the use of (21) and (22) where various grid sizes are chosen in order to achieve the convergence of the solution. It may be mentioned that the convergence has been achieved with desired degree of accuracy for a grid size of 41×41. Final results for the desired quantities are exhibited through Figures 3–13 in order to estimate them quantitatively.

Figure 3 illustrates the results for the velocity profile of the flowing blood at three specific locations of the stenosed artery at a particular instant of $t = 1\,\text{s}$. The curves are found to be decreasing from their maximum at the axis as one moves away from it and finally they become zero on the wall surface. The axial flow velocity appears to be enhanced most at the onset ($z = 4.5\,\text{mm}$) of the stenosis while a reduction is noted the moment the flow becomes upstream at a location of $z = 12\,\text{mm}$, and thereafter, at the overlapping region ($z = 15.75\,\text{mm}$) of the stenosis, the flow velocity is increased further. Also, the results corresponding to a normal arterial flow ($\tau_m = 0$) at the same instant of time coincides with those of the topmost curve present in this figure which remains invariant with respect to the axial position of the artery. Thus, the overlapping shape of the stenosis in the arterial lumen affects the flow considerably.

The results for the distribution of the streaming blood throughout the stenosed artery are presented in Figure 4 for three different time periods. For all the curves, as anticipated, the flow velocity diminishes from its maximum in the nonstenotic region until the stenosis attains its maximum height, thereafter, it increases up to the overlapping zone followed by a gradual

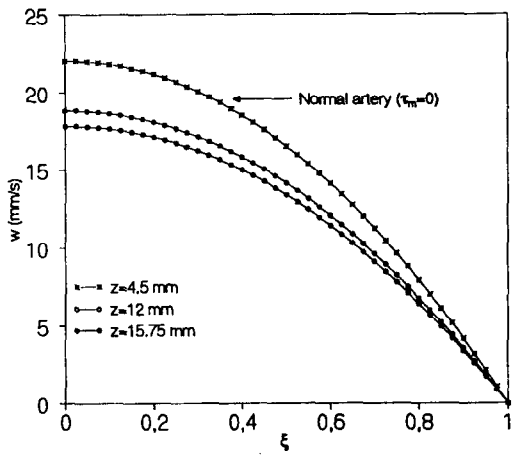

Figure 3. Flow velocity profile at three specific locations of the stenosed artery at $t = 1\,\mathrm{s}$ ($\tau_m = 0.4a$).

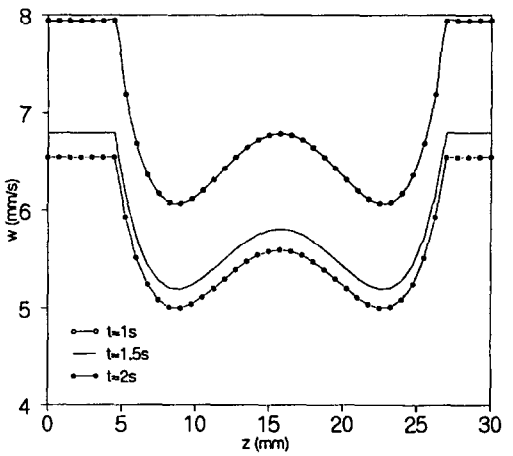

Figure 4. Velocity distribution of the stenotic flow at different time periods ($\tau_m = 0.4a$, $\xi = .8$).

decrease downstream until the stenosis gets back its maximum height and finally it increases at the offset of the stenosis. The peaks which appear in all the curves in the constricted area of the stenosed artery are formed at the overlapping region of the stenosis under consideration where the constrictions assume minimum. Regarding its variation with time one may note that the curves are shifted towards the origin as time progresses which is reflecting very closely the outline of the time-dependent stenosis as shown in Figure 2.

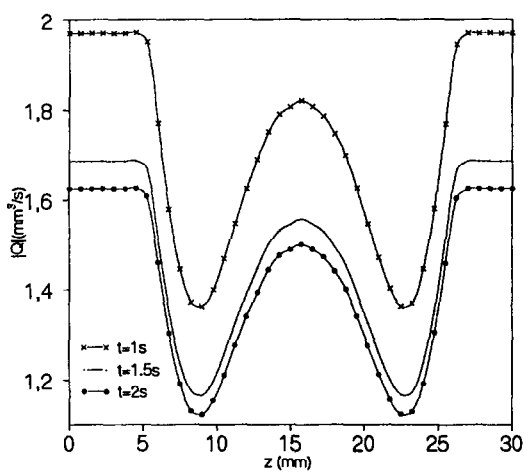

Figure 5. Flux distribution for different time periods ($\tau_m = 0.4a$).

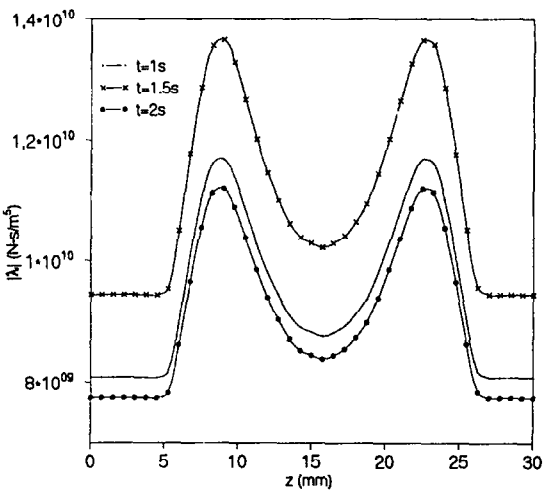

Figure 6. Distribution of resistive impedance for different times ($A_0 = 500\,\mathrm{kg\,m^{-2}\,s^{-2}}$, $A_1 = 0.2A_0$, $\tau_m = 0.4a$).

The results of Figure 5 record the distributions of the flow rate over the stenosed artery for different time periods. The flux diminishes at the onset of the stenosis until the constrictions approach their maxima and, thereafter, increases sharply until the constrictions assume minima, while in the nonstenotic portions of the arterial segment, the flux distribution is higher and remains invariant. The nature of the flow rate curves is analogous to that of the velocity distribution as shown in Figure 4. Here, also, the curves do shift towards the origin with time advancement. Thus, one may report in this connection that the rate of blood flow enhances or reduces to some extent with the arterial length in the stenosed area, depending upon whether the cross-section of the arterial segment concerned increases and decreases, respectively. Thus,

the variation of the flow rate along the arterial length appears to be noteworthy, owing to the fact that the flow rate depends on the variable radius of the artery in the constricted area.

The distributions of the resistance to flow or impedance over the stenosed arterial segment under study for different time periods are shown through the results exhibited in Figure 6. Unlike the behaviour of the flow rate, the resistive impedance gets enhanced at the onset of the stenosis until its maximum constriction, and thereafter, declines sharply as the constrictions assume minimum, while in the nonstenotic portions of the arterial segment the resistance experienced by the flowing blood is considerably lower and remains invariant there. Two peaks appear at the specific locations where the arterial narrowing approach maximum. The observation made in the present figure are believed to be quite justified in the realm of physical concepts if one examines the result presented in Figure 5. It may be remarked from the results of these two figures that the rate of blood flow under stenotic conditions depends entirely on the magnitude of resistive impedance it experiences, or in other words, the flow rate becomes inversely proportional to the impedance arising out of the stenotic flow *in vivo*. It is also worth mentioning that the new stenosis geometry introduced in the present study potentially contributes to such an important observation. Moreover, its variation with time is mostly influenced by the pulsatile pressure gradient giving rise to systolic and diastolic pressure.

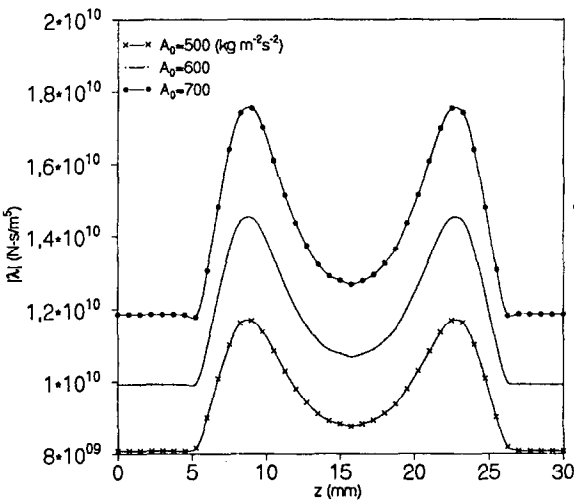

Figure 7. Resistance to flow for various amplitudes of the pressure gradient at $t = 1\,\mathrm{s}$ ($\tau_m = 0.4a$, $A_1 = 0.2A_0$).

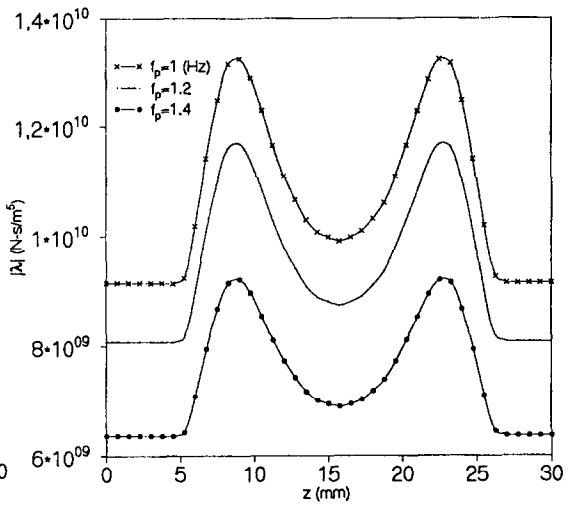

Figure 8. Resistive impedances for various angular frequencies at $t = 1\,\mathrm{s}$ ($A_0 = 500\,\mathrm{kg\,m^{-2}\,s^{-2}}$, $A_1 = 0.2A_0$, $\tau_m = 0.4a$).

Figure 7 includes the results for the variations of the resistive impedances distributed over the arterial segment, with different amplitudes of the pressure gradient at a particular instant of $t = 1\,\mathrm{s}$. The resistive impedances are observed to be increasing at a uniform rate with the increase in the amplitude of the pressure gradient, which means that the resistance to flow becomes linearly proportional to the constant amplitude of the pressure gradient. In all the curves of the present figure, the peaks appear at the specific locations where the arterial cross-sections assume minimum irrespective of the magnitudes of the pressure gradient.

Unlike the behaviour of the results shown in Figure 7, the resistive impedances are recorded to be diminishing considerably with increasing pulse frequency of the pressure gradient as displayed in Figure 8 at the same instant of $t = 1\,\mathrm{s}$. The rate of decrease of the resistance to flow is small when the pulse frequency changes from 1 Hz to 1.2 Hz, but it diminishes at a higher rate for a further increase of the frequency from 1.2 Hz to 1.4 Hz. Thus, analysing the results of these two figures, one can conclude that the resistive impedances vary directly with the amplitudes of the pressure gradient giving rise to systolic and diastolic pressure and inversely with the pulse frequency.

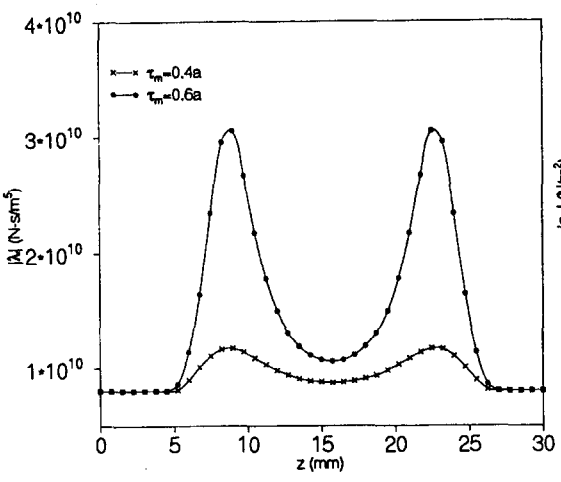

Figure 9. Effect of the severity of the stenosis on the resistive impedances ($A_0 = 500\,\mathrm{kg\,m^{-2}\,s^{-2}}$, $A_1 = 0.2A_0$, $\tau_m = 0.4a$).

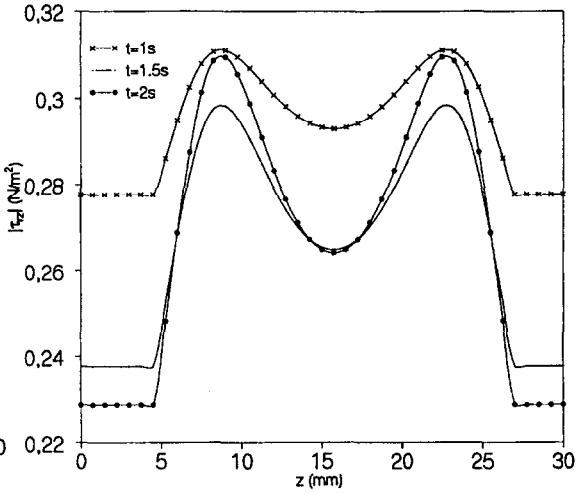

Figure 10. Distribution of wall shear stress over the arterial segment for different times ($A_0 = 500\,\mathrm{kg\,m^{-2}\,s^{-2}}$, $A_1 = 0.2A_0$, $\tau_m = 0.4a$).

Figure 9 illustrates the distribution of the impedance over the stenosed arterial segment and its variation with the thickness of the stenosis at an instant of $t = 1\,\mathrm{s}$. The two curves correspond to two different heights of the overlapping stenosis. It may be noted that the resistance to flow is greatly enhanced even for a slight increment of the height of the stenosis. In other words, if the severity of the stenosis is raised from 40% to 60% the resistive impedance becomes higher and it is found to develop more (with an increase of about 26%) at those critical locations where the arterial cross-sections are minimum. The observation made in the present figure agrees qualitatively well with that of Srivastava [23] who studied the behaviour of the couple stress fluid representing blood under stenotic condition as a function of difference in the geometry of the stenosis, disregarding the arterial wall motion. As his results were displayed in a dimensionless form, they could not be reproduced directly in the present figure and hence, no quantitative comparison to, or validation of, the results of our study could be made. Thus, one may conclude that if constriction grows, then resistance grows up fast, with or without the arterial wall motion.

The results of the wall shear stress distributed over the arterial segment for different time periods are presented in Figure 10. The wall shear stress appears to gain its maximum magnitude at the critical sites where the arterial constrictions assume their maxima, while a reduction of its magnitude is noted at the overlapping region of minimum constriction. It may be of importance to note that the wall shear stress is distributed symmetrically over the stenotic region for all time under consideration about the same critical points as mentioned above and their pulsatile behaviour with time is greatly influenced by the input pressure gradient like the nature of those presented in Figure 6. Such distribution of the wall shear stress plays a significant role in detecting the aggregation sites of platelets as suggested by Fry [24] that the growth and the deterioration of the endothelial cells are closely related to the generation of the shear stresses on the arterial walls. For normal artery, that is, in the absence of any arterial constriction, the magnitudes of the wall shear stresses in all the time-dependent curves are reduced considerably and they remain invariant throughout the arterial segment under consideration along the lines joining the respective results for the proximal and distal portions as evident from the figure, and thereby, the effect of stenosis on the wall shear stress can be measured quantitatively.

Figure 11 exhibits the distribution of the wall shear stress in the arterial system under study with a variance of the amplitudes of the pressure gradient at a particular instant of $t = 1\,\mathrm{s}$. As the amplitude (both for the constant part and the pulsatile component) of the pressure gradient increases, the wall shear stresses appear to be diminishing to some extent throughout the artery unlike the behaviour of the resistive impedances presented in Figure 7. It is quite feasible that with

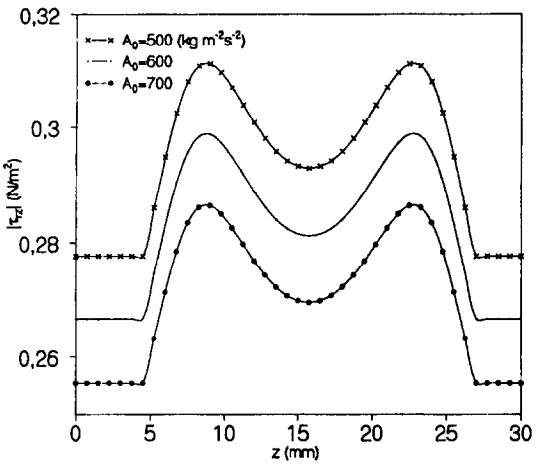

Figure 11. Wall shear stress distribution for various amplitudes of the pressure gradient at $t = 1\,\mathrm{s}$ ($\tau_m = 0.4a$, $A_1 = 0.2A_0$).

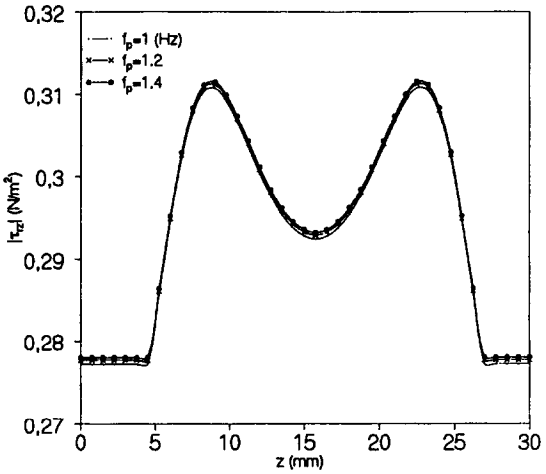

Figure 12. Wall shear stress distribution for various angular frequencies at $t = 1\,\mathrm{s}$ ($\tau_m = 0.4a$, $A_0 = 500\,\mathrm{kg\,m^{-2}\,s^{-2}}$, $A_1 = 0.2A_0$).

the increasing pressure gradient, the resistance to flow enhances its magnitude to a considerable extent owing to the reduced flow throughout the stenosed artery, and thereby, the wall shear stress diminishes, following a contraction of the arterial wall. Moreover, its variation with the pulse frequency (as shown in Figure 12) at the same instant of time is meagre although there is a trend of slight increase with increasing pulse frequency.

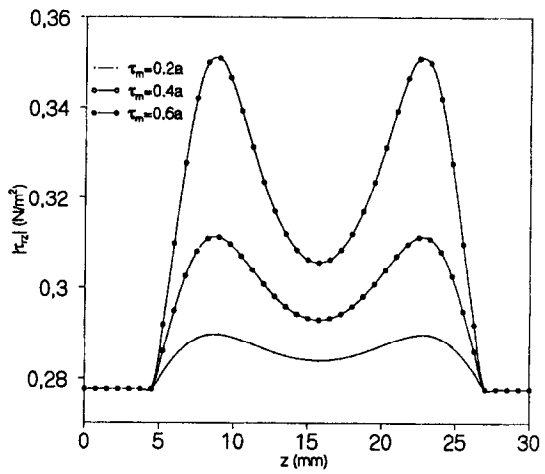

Figure 13. Effect of the severity of the stenosis on the wall shear stresses at $t = 1\,\mathrm{s}$ ($A_0 = 500\,\mathrm{kg\,m^{-2}\,s^{-2}}$, $A_1 = 0.2A_0$).

Finally, the effects of the severity of the stenosis on the wall shear stress has been pointed out through the results plotted in the concluding Figure 13 at $t = 1\,\mathrm{s}$. The severity of the stenosis can be visualized by changing the maximum height of the stenosis. One may record that the wall shear stress is enhanced appreciably throughout the stenotic region when the height of the stenosis is kept on increasing. In other words, if the severity of the stenosis is raised from 20% to 40% the wall shear stress becomes higher and higher, which is found to develop more at the critical locations where the arterial narrowings are maximum. Thus, the severity of the stenosis (overlapping) affects the wall shear stress characteristics significantly. The peaks observed in the wall shear stress characteristic are believed to cause severe damage in the endothelial cells of the arterial system which help determining the aggregation sites of the platelets.

CONCLUDING REMARKS

A mathematical model for blood flow in a stenosed arterial segment has been developed where the time-dependent stenosis has been given a new overlapping shape. The analysis has been carried out with special emphasis upon the experimentally established viscoelastic properties of the flowing blood and the deformability of the arterial wall. The flow mechanism has been made, governed by a pulsatile pressure gradient.

Salient observations of this study are listed below:

(1) The flow velocity diminishes downstream from its value at the onset of the stenosis and further increases upstream towards the overlapping region.
(2) The flow velocity diminishes or increases depending upon whether the arterial constrictions assume maximum or minimum, respectively.
(3) The nature of the flow velocity in the unsteady state reflects very closely the outline of the time-dependent stenosis.
(4) The flow rate becomes inversely proportional to the resistive impedance arising out of the stenotic flow *in vivo*.
(5) The peak resistances to flow occur where the arterial narrowings approach maximum.
(6) Resistive impedance becomes directly proportional to the amplitude of the pressure gradient and inversely with the pulse frequency.
(7) The severity of the overlapping stenosis affects the resistive impedance significantly, that is, the more the severity, the more is the amount of resistance to flow.
(8) The wall shear stress increases or decreases, depending upon whether the arterial cross-section diminishes or increases, respectively.
(9) The wall shear stress becomes inversely proportional to the amplitudes of the pressure gradient.
(10) The severity of the stenosis has significant effect on the wall shear stress in such a way that it develops more at the maximum constricted locations than all other sites of the artery.
(11) The time variations of the resistive impedances and the wall shear stresses are mostly influenced by the pulsatile pressure gradient.

REFERENCES

1. D.F. Young, Effect of a time-dependent stenosis on flow through a tube, *J. Engng. Ind., Trans. ASME* **90**, 248–254 (1968).
2. J.H. Forrester and D.F. Young, Flow through a converging diverging tube and its implications in occlusive vascular disease, *J. Biomech.* **3**, 297–316 (1970).
3. J.S. Lee and Y.C. Fung, Flow in locally constricted tubes at low Reynolds numbers, *J. Appl. Mech.* **37**, 9–16 (1970).
4. D.F. Young and F.Y. Tsai, Flow characteristics in models of arterial stenosis—I. Steady flow, *J. Biomech* **6**, 395–411 (1973).
5. J.C. Misra and S. Chakravarty, Flow in arteries in the presence of stenosis, *J. Biomech.* **19**, 907–918 (1986).
6. D. Hershey, R.E. Byrnes, R.L. Deddens and A.M. Rao, Blood rheology: Temperature dependence of the Power law model, Presented at the *A.I.Ch.E. Meeting*, Boston, MA, (December 1964).
7. C.E. Huckaba and A.N. Hahn, A generalised approach to the modelling of arterial blood flow, *Bull. Math. Biophys.* **30**, 645–662 (1968).
8. S.E. Charm and G. Kurland, Viscometry of human blood for shear rates 0–100,000 $\sec^{-1}$, *Nature* **206**, 617–618 (1965).
9. R.L. Whitemore, *Rheology of the Circulation*, Pergamon Press, New York, NY, (1968).
10. C.D. Han and B. Barnett, Measurement of the rheological properties of biological fluids, In *Rheology of Biological Systems*, (Edited by H.L. Gabelnick and M. Litt), p. 195, Charles C. Thomas, Illinois, (1973).
11. J.B. Shukla, R.S. Parihar and B.R.P. Rao, Effects of stenosis on non-Newtonian flow of the blood in an artery, *Bull. Math. Biol.* **42**, 283–294 (1980).
12. S. Chakravarty, Effects of stenosis on the flow behaviour of blood in an artery, *Int. J. Engng. Sci.* **25**, 1003–1018 (1987).
13. S. Chakravarty and A. Datta, Effects of stenosis on arterial rheology through a mathematical model, *Math. Comp. Modelling* **12**, 1601–1612 (1989).

14. S. Chakravarty and A. Datta, Dynamic response of stenotic blood flow in vivo, *Math. Comp. Modelling* **16**, 3–20 (1992).
15. A. Lessner, J. Zahavi, A. Silberberg, E.H. Frei and F. Dreyfus, The viscoelastic properties of whole blood, In *Theoretical and Clinical Hemorheology*, (Edited by H. Hartert and A.L. Copley), pp. 194–205, Springer-Verlag, New York, NY, (1971).
16. G.B. Thurston, Frequency and shear rate dependence of viscoelasticity of human blood, *Biorheology* **10**, 375–381 (1973).
17. A.C. Burton, Introductory text, *Physiology and Biophysics of the Circulation*, Year Book Medical Publisher, Chicago, IL, (1966).
18. D.U. von Rosenberg, *Methods for the Numerical Solution of Partial Differential Equations*, Elsevier, New York, NY, (1969).
19. V.I. Krylov and N.S. Skoblya, *A Handbook of Methods of Approximate Fourier Transformation and Inversion of Laplace Transformation*, Mir Publisher, Moscow, (1977).
20. D.A. McDonald, *Blood Flow in Arteries*, Edward, (1974).
21. W.R. Milnor, *Hemodynamics*, Williams and Williams, Baltimore, MD, (1982).
22. G.B. Thurston, Effects of viscoelasticity of blood on wave propagation in the circulation, *J. Biomech.* **9**, 13–20 (1976).
23. L.M. Srivastava, Flow of couple stress fluid through stenotic blood vessels, *J. Biomech.* **18**, 479–485 (1985).
24. D.L. Fry, Acute vascular endothelial changes associated with increased blood velocity gradient, *Circulation Res.* **22**, 165–197 (1968).